 DOI: 10.1051/metrology/201717001

New optical power sensors using pyrolytic graphite

Patrick Pinot[1,*] and *Zaccaria* Silvestri[1]

[1]Conservatoire national des arts et métiers, Laboratoire commun de métrologie, 93210 La Plaine Saint-Denis, France

Abstract. We present two experimental configurations based on a repulsion force acting on a piece of pyrolytic carbon (PyC) in a magnetic induction generated by a magnet array to measure a laser power in the range from a few milliwatts to a few watts. The levitation configuration consists in measuring the levitation height change of the PyC sheet related with the optical power irradiating its surface. The weighing configuration consists in measuring the mass change corresponding to a magnetic repulsion force change acting on a piece of PyC placed on a balance pan and irradiated by a laser beam. The quantities affecting the measurement results have been identified. Examples of measurement results are given. The relative uncertainty of optical power measurement is less than 10% for the first experimental set-up and around 1% for the second one. The wavelength dependence on power response of this device has been quantified. The two PyC-based devices presented in this paper offer a new technique for measuring optical power.

1 Introduction

We present two set-ups using a pyrolytic carbon (PyC) sheet to measure a laser power in the range from 10 mW to 1 W. These elementary devices are based on a small plate of PyC placed in a magnetic flux density generating a repulsion force on the PyC sheet. This force varies when the sheet is irradiated by a laser beam and is related with the optical power. This leads to an alternative to traditional power meters based on thermal measurement techniques via the Stefan-Boltzmann law and photon-electron interaction.

The first experimental configuration presented in a previous paper [1] consists in using the levitation effect of the PyC sheet above a magnet array. Due to the periodicity of the magnetic flux density, the position of the levitated PyC sheet is steady but its levitation height is modified when the PyC surface is irradiated by a laser beam. This leads to potential energy change:

$$\Delta E_t = E_0 \frac{\Delta d_t}{d_0} \qquad (1)$$

where Δd_t is the levitation height change and E_0 is the potential energy of the PyC sheet at the initial levitation height d_0. The power response in terms of levitation height *versus* irradiation power is sufficiently linear, sensitive and reproducible to be used as a laser power sensor. The height change Δd_t depends on the exposure time t_{exp}. It appears to be a suitable measurement parameter for establishing a relation with the irradiating laser power. Several physical quantities can affect the measurement results. In particular, this levitation configuration is very sensitive to mechanical vibration, draughts and temperature fluctuation.

The second configuration presented in another previous paper [2] consists in detecting the repulsion force change between the PyC sheet and the magnet array. In this case, the PyC sheet is placed on the pan of a mass comparator (Mettler Toledo AX206) and the magnet array is held above the PyC sheet at a short distance. The measurement principle is based on the force change expressed in terms of mass through the mass comparator when the PyC surface is irradiated by a laser beam. Thus, there is an equivalence of the potential energy change and the mass change Δm_t as follows:

$$\Delta E_t = E_0 \frac{\Delta m_t}{m_0} \qquad (2)$$

with the same PyC piece ($m_0 = 0.41$ g), and for an identical position and fixed distance ($d_0 \approx 0.4$ mm) between the PyC surface and the magnet array as in the levitation configuration, we obtain a mass change Δm_t of about 1 mg in the weighing configuration which is equivalent to a height change Δd_t of 1 µm in the levitation configuration. The weighing configuration is mainly sensitive to the ambient temperature fluctuation, but the linearity and reproducibility are somewhat better in the power range from 0.2 W to 1 W in this configuration than in the levitation one. However, energy is dissipated in ambient air, which leads to a slight drift being observed in the mass indication by the mass comparator due to thermal effects. This drift can be easily corrected for.

First results are very encouraging. This confirms the feasibility of new laser power sensors using diamagnetic repulsion which appear interesting for applications in metrology, in industry or in technology development. The need to measure high power lasers accurately in

* Corresponding author: patrick.pinot@cnam.fr

Article available at http://cfmetrologie.edpsciences.org or https://doi.org/10.1051/metrology/201717001

real-time in laser manufacturing operations has been highlighted [3].

In this paper, the experimental set-up for the levitation configuration is described in subsection 2.1. The magnetic levitation is presented in subsection 2.2. Thermal effects are discussed in subsection 2.3 and examples of results presented in subsection 2.4. The second set-up for the weighing configuration is described in subsection 3.1. The buoyancy affecting the weighing is discussed in subsection 3.2. Thermal effects affecting the measurement stability are presented in subsection 3.3 after which examples of measurement results are discussed in subsection 3.4.

2 Levitation configuration

2.1 Experimental set-up

Figure 1 shows the experimental set-up for the levitation configuration. This device has been improved by the addition of a damping system compared with the first prototype described in a previous paper [1].

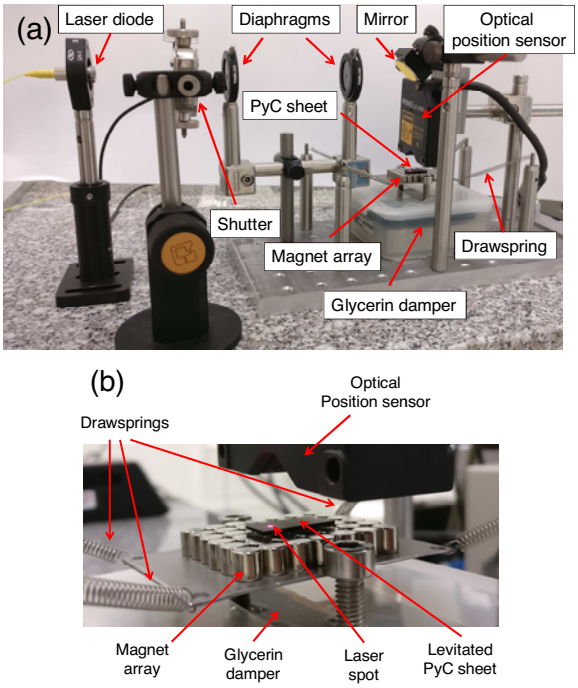

Fig. 1. Photographs of the experimental set-up in the levitation configuration. (a) Overview of the set-up (in this case, the laser under test is a laser diode emitting 3 mW at 635 nm; (b) Close-up of the magnet array on the damping device and levitated PyC sheet.

The levitation configuration is a very simple device which consists of a magnet array, a sheet of pyrolytic carbon, two diaphragms, a mirror, a shutter and a laser displacement sensor.

The horizontal magnet array is composed of (5×7) cylindrical magnets of diameter and height 6 mm. To attenuate the vibration effect, the magnet array is hung with four springs and is coupled with an horizontal aluminum plate immerged in glycerin to damp the device.

The dimensions of the PyC piece are 24 mm × 8 mm × 1 mm.

The two diaphragms (∅ 1.5 mm and 1.0 mm) are used to limit the size of the laser spot and to ensure always the same area of the PyC surface is illuminated.

Once the horizontal laser beam has passed through the two diaphragms, it is reflected and directed vertically downwards onto the PyC surface.

The shutter is placed between the laser head and the first diaphragm to control the exposure time.

The laser displacement sensor (Keyence LC-2420) is used to measure the height change of the PyC sheet when its surface is irradiated.

2.2 Magnetic field

Several configurations have been studied corresponding to different stable positions of the PyC sheet where its potential energy is the lowest. Given both the sizes of the PyC sheet and of the magnet array, there are only six stable levitation positions. Each PyC position change necessarily entails position changes of the Keyence sensor laser spot and of the irradiation spot of the laser beam under test. Consequently, there is one metrological characterization valid only for one position. Each PyC position is identified as “position X” where X is an order number.

Figure 2 shows a photograph of the PyC sheet levitated at about 0.4 mm above the magnet array surface.

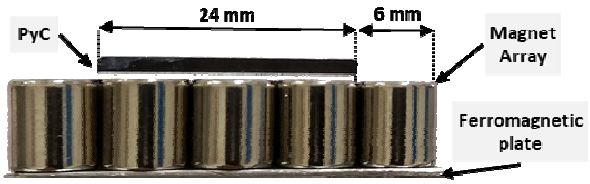

Fig. 2. Photograph of the PyC sheet levitated above the magnet array (position 1).

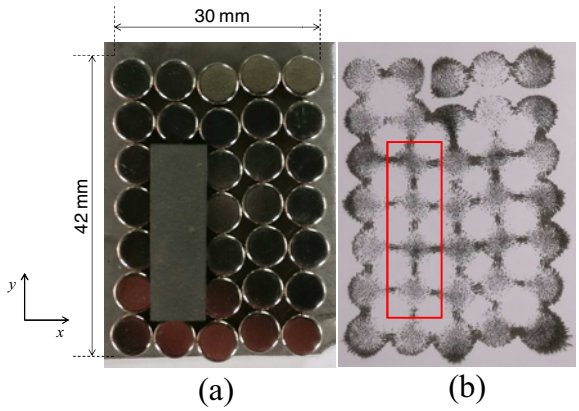

Fig. 3. Photographs of the magnet array:
a) Arrangement of the (5×7) 6 mm-diameter magnets with the PyC piece levitated at position 1;
b) Same area as shown in Fig 3a covered with a sheet of white paper sprinkled with iron filings. The rectangle represents the PyC position 1 in this example.

 DOI: 10.1051/metrology/201717001

The photograph of Figure 3.a shows the magnet array with the PyC sheet levitated at one of its stable positions. As expected and shown by the iron filings sprinkled on white paper placed on the magnet array surface in the example of Figure 3.b, the arrangement of the (5×7) 6 mm-diameter magnets induces a 2D periodicity of the magnetic field above the magnet array with a spatial period of about 6 mm.

However, one can see in Fig 3b that the periodicity is not perfect due to misalignments of the magnets. This leads to local heterogeneities of the magnetic field. They can affect the PyC response to an irradiation power according to the levitation position above the magnet array in the horizontal plane.

2.2 Surface temperature

To evaluate the risk of any local intense heat and the necessity to limit the exposure time for higher laser powers, thermal tests were carried out using a thermal imaging camera Optris PI (OPTPI16-O31T900).

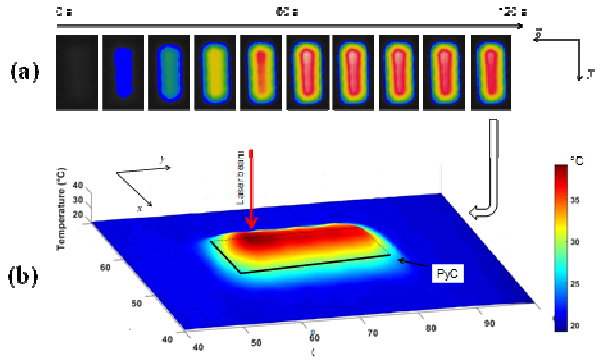

Fig. 4. False color images taken by the thermal imaging camera Optris PI (OPTPI16-O31T900).
a) Sequence of the levitated PyC surface extracted over 120 s during irradiation by the 1064 nm laser beam at 0.9 W;
b) Temperature distribution 3D-image after irradiating the PyC surface for 120 s at a laser power of 0.9 W (corresponding to the last image of the sequence).

Figure 4.a shows a sequence of successive false color images, taken every 12 s, of the temperature measurement of the PyC surface illuminated by a 1064 nm laser beam of 0.9 W. The temperature increase seems to tend towards a plateau at about 40 °C after the surface has been irradiated for t_{exp} =120 s. This results from the exceptional thermal properties of this material which presents a high anisotropy. The irradiation induces a photothermal effect which reduces the diamagnetism of the material [4].

Figure 4.b shows a false color image of the PyC surface extracted from a thermal camera recorded after 120 s of irradiation by the 1064 nm laser beam at 0.9 W. The temperature imaging threshold was chosen at 22 °C corresponding to the contour line. The ambient air temperature was 21 °C. The analysis of images taken over 120 s irradiation shows that the temperature diffusion from the irradiated point at one of the PyC sheet ends to the other end is not instantaneous. In addition, it seems in Figure 4.b that a temperature increase in the horizontal plane over the PyC edges could correspond either to an imaging artifact (blurring effect) or more probably to a heat exchange with the ambient air close to the PyC piece.

In other words, this means that there is a heat exchange with the ambient air close to the PyC sheet leading to a balance between absorbed energy (thermally excited electrons by irradiation) and emitted energy (heat transferred to the air).

2.3 Result and discussion

Figure 5 shows examples of curves obtained from the recorded data for position 2 for eleven values of irradiation power P_{irr} at a wavelength of about 1064 nm. The exposure time t_{exp} was limited to 20 s and the ambient air temperature was (22.7 ± 0.2) °C. These examples are particular because the displacement change *versus* exposure time is negative and relatively small. This means that the levitation height increases with the exposure time for position 2. In addition, a plateau is reached after the PyC surface has been irradiated for about 10 s. For the other positions, the displacement change is positive and the plateau is ten times higher for the same optical power. Consequently, the device is much more sensitive to the irradiating optical power for the other positions than for position 2, but the plateau is reached after 60 s of irradiation instead of 10 s.

Nevertheless, the experimental results showed in Figure 5 can be used to determine the metrological specifications of the PyC-based sensor for position 2. Figure 6 shows the graphical representation of the levitation height change after an exposure time of 20 s for the different optical powers in Figure 5. Figure 6 also shows that the photo-response of the sensor is not linear in the range 100-1000 mW. The best fit is obtained by using a second-order polynomial regression. However, the sensor response can be considered linear within two sub-ranges 100-400 mW and 400-1000 mW. This point is observed for all positions.

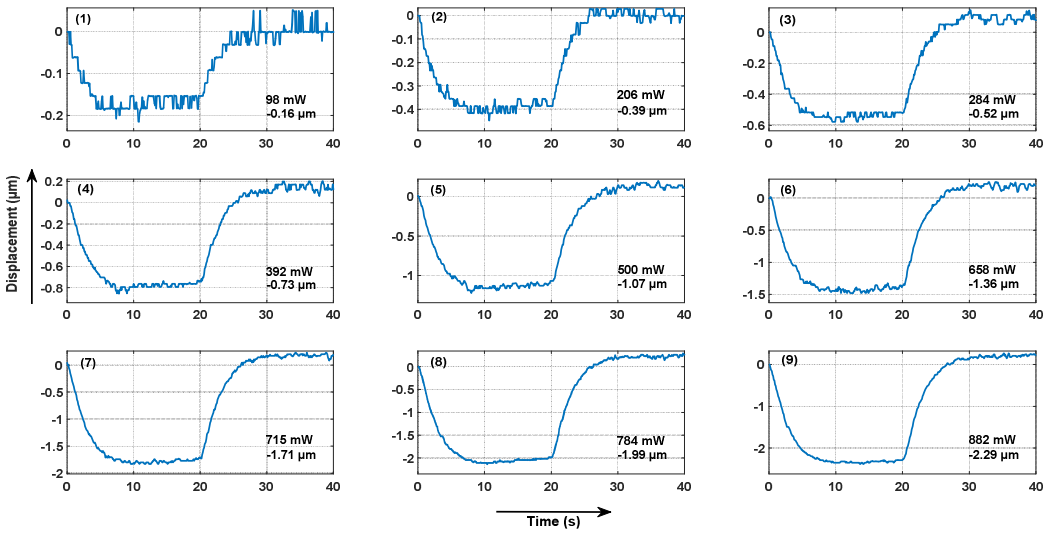

Fig. 6. Examples of curves obtained from experimental data for position 2 of the PyC sheet. The maximum exposure time is 20 s. The irradiation power P_{irr} and the maximum differential displacement Δd_{20} are indicated on each graph.

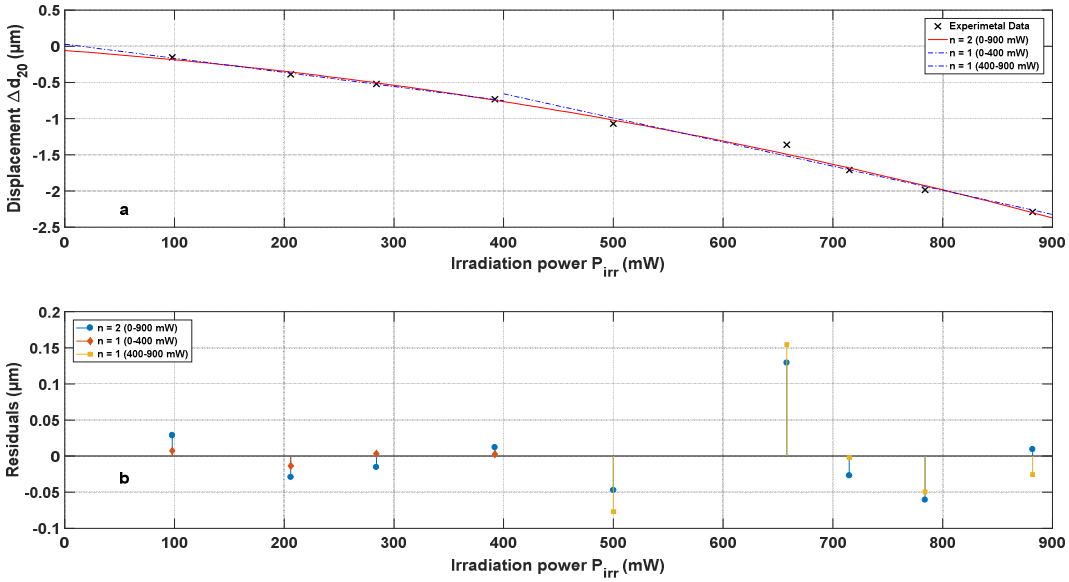

Fig. 5. Graphical representation from experimental data in Figure 5. a) displacement value Δd_{20} *versus* irradiation power P_{irr}; curve from a second-order polynomial fit (solid line) and linear fits (dotted lines); b) residuals for every polynomial fit.

2.4.1 Background noise

Note that the sensitivity and the signal-to-noise ratio depend on the PyC configuration. To appreciate this point, just compare the example for two different positions in Figure 7 for P_{irr} = 46 mW with an exposure time of 60 s at 1064 nm. Curves 7a and 7b are obtained for positions 3 and 4 of the PyC sheet, respectively.

For low power when the height changes either during the irradiation or after closing the shutter are quite low, the background noise is preponderant. There are three main sources of noise, one due to the quantization noise of the Keyence displacement sensor, another due to the air-conditioning system and a third one due to ground vibrations. From recordings of Δd_t when the PyC surface is not irradiated, the standard deviation of the signal is $u_{cr} \approx 0.044$ µm when the air conditioning system is running while it is $u_{cs} \approx 0.029$ µm when it is stopped.

Assuming that:

- these values of standard deviation are the quadratic sum of the standard deviations u_q, u_c and u_v respectively associated with the three sources of noise;
- the quantization noise characterized in terms of uncertainty corresponds to the uncertainty associated with resolution following a uniform probability distribution;

we can deduce the following approximate values: $u_q \approx 0.003$ µm, $u_c \approx 0.033$ µm and $u_v \approx 0.029$ µm. This means that the contribution of quantization noise is negligible compared with the two other sources of which the contribution is almost equivalent. Therefore, all the measurements were carried out without air-conditioning.

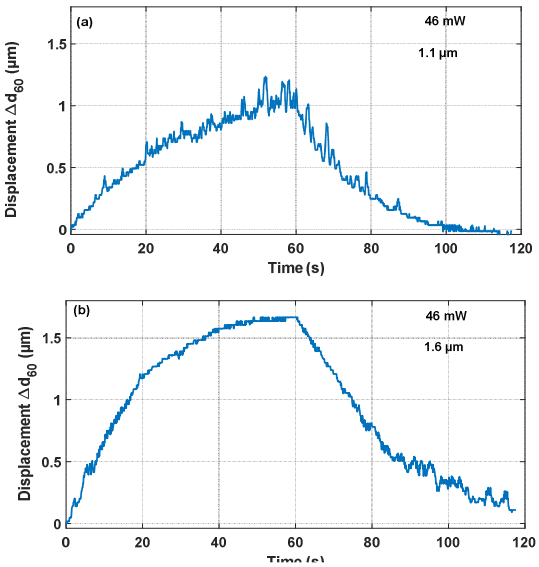

Fig. 7. Curves for two different PyC positions obtained from experimental data with an exposure time of 60 s with a 1064 nm laser beam at 46 mW; (a) position 3; (b) position 4.

2.4.2 Sources of error and uncertainties

In this experiment, there are several sources of error due to parameters affecting the measurement which must be taken into account in the uncertainty budget.

In addition to the uncertainty component due to the repeatability of the PyC sensor measurements in terms of type A evaluation of uncertainty [5], the main contributions of uncertainty (type B evaluation [5]) for this study come from:
- the power meter which was not calibrated and whose measurement position was not well defined;
- the area of the laser spot and its position on the PyC surface;
- the background noise due to vibrations;
- the local inhomogeneities of the magnetic field;
- the size and the horizontal position and orientation of the PyC sheet over the magnet array;
- the surface quality and the absorption coefficient of the PyC;
- the position of the displacement Keyence sensor spot on the PyC surface;
- the method in terms of exposure time, sampling time and linearization parameter.

Several contributions of these uncertainty components are made negligible by the use of diaphragms and for a fixed position of the PyC sheet. The sensitivity of the sensor could be improved by choosing the best position and size of the PyC sheet adapted to the magnetic field distribution. In addition, the experiment in this configuration could be greatly improved by protecting the PyC sheet against ground vibrations and temperature fluctuations to improve the signal-to-noise ratio.

The calibration of this device could consist in determining the calibration coefficient $\beta(T, \lambda, t_{exp}, P)$ which depends on the ambient air temperature range T, the laser wavelength range λ, the exposure time t_{exp} and the laser power range P used in expression (3) linking the laser power P_{irr} to the levitation height change measured over a short irradiation time t_{exp}:

$$P_{irr} = \beta \Delta d_t + \gamma \quad (3)$$

For instance, with T = (22.7 ± 0.2) °C, $\lambda \approx 1$ µm, t_{exp} = 5 s and P = [100 mW; 400 mW], we obtain: $\beta \approx 187$ mW·µm^{-1} and $\gamma \approx 0$ for position 5.

From these considerations, it seems realistic to be able to develop a laser power sensor using diamagnetic levitation calibrated with a relative measurement uncertainty of few percent or less than 10% in any case. Note that tests made at 532 nm seem to show that the PyC photo-response to an irradiation power of this experimental device depends also on the laser wavelength. Other tests made at 635 nm have shown that the discrimination threshold for the positions given a sensitivity β larger than 100 mW·µm^{-1} is about 3 mW for an exposure time of around 60 s.

3 Weighing configuration

3.1 Experimental set-up

Figure 8 shows photographs of the experimental set-up for the weighing configuration.
The device uses the same magnet array, PyC piece, diaphragms, mirror and shutter as those used in the levitation configuration but, in addition, a mass comparator is used to measure the equivalent mass change corresponding to the magnetic interaction force change between the magnet array and the PyC piece when it is irradiated by a laser beam.

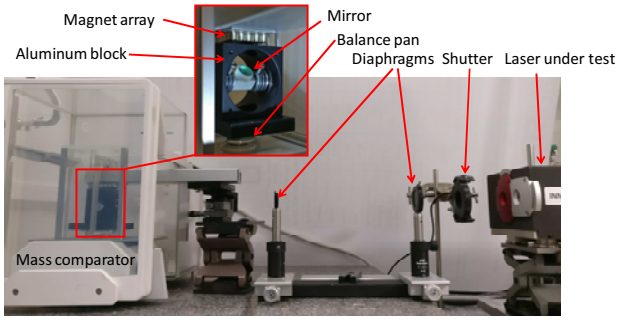

Fig. 8. Photographs of the experimental set-up for the weighing configuration.

In the weighing configuration, the magnet array is horizontally fixed to an aluminum arm linked to a 3D translation stage to adjust its position above the PyC sheet. The PyC sheet piece is glued to an aluminum block placed on the balance pan. The mirror is fixed at 45° in the aluminum block to reflect vertically the horizontal laser beam onto the PyC surface after it has passed through two diaphragms.

3.2. Buoyancy

The mass m of the device placed on the balance pan is about 200 g (aluminum block+ mirror+ PyC sheet). The main part (98%) of this mass comes from the aluminum block (density ρ_{Al} = 2700 kg·m^{-3}). The buoyancy in terms of mass Δm_a is given by:

$$\Delta m_a = -m\frac{\rho_a}{\rho_{Al}} \qquad (4)$$

where ρ_a is the density of moist air.

The buoyancy of the aluminum block is about -89 mg for an ambient air temperature of about 20 °C and a conventional air density of 1.2 kg·m^{-3}.

The density of moist air ρ_a can be calculated using the formula recommended by the OIML [6]:

$$\rho_a = \frac{0{,}34848p - 0{,}009H\exp(0{,}061T)}{273{,}15+T} \qquad (5)$$

where p is the pressure expressed in hPa, T the temperature expressed in °C and H the relative humidity expressed in %.

The relative sensitivity coefficients [6] of the air parameters are as follows:

$$\frac{1}{\rho_a}\frac{\partial\rho_a}{\partial T} = -3.4\times10^{-3} \quad \mathrm{K}^{-1};$$
$$\frac{1}{\rho_a}\frac{\partial\rho_a}{\partial p} = +1\times10^{-5} \quad \mathrm{Pa}^{-1};$$
$$\frac{1}{\rho_a}\frac{\partial\rho_a}{\partial H} = -1 \quad \%. \qquad (6)$$

For our device, the measurement indication is not the "absolute" mass, but the mass change over exposure time t_{exp} or over recording time t_{max}. We choose as criterion that the slope of the buoyancy mass change over one second must be less than 1 µg/s. This means that the relative air density change must be less than 1.3×10^{-3} for an exposure time of 60 s. In these conditions, the buoyancy change has no significant effect on the mass change measurements. Using expression (6) we obtain the following limits of the variation of ambient conditions for 60 s exposure:

- $\partial T/\partial t = \pm 0.18$ °C/min ;
- $\partial P/\partial t = \pm 0.68$ hPa/min ;
- $\partial H/\partial t = \pm 7.7$ %/min.

Since all the experiments for this study have been carried out in these environmental limits, we need not apply any buoyancy correction.

3.3 Instability of weighing due to temperature

In the weighing configuration, as shown in Figure 9, the maximum temperature of the PyC surface reaches about 25.3 °C at ambient air temperature of about 21.9°C when the PyC surface is illuminated in the same conditions as that of the levitation configuration. Corrected for the air temperature slope, the temperature change of the PyC surface is only 3.4 °C. This is very small compared with the 16 °C measured for the levitation configuration. Two reasons can explain this difference. First, the aperture and the position of the diaphragms D1 and D2 were not exactly the same in the two configurations, while they limit the same optical power irradiating the mirror M1 in the weighing configuration. Secondly, it appears that a significant amount of energy is dissipated through the two contact zones with the C profile despite the thin insulating sheets. This assumption is confirmed in Figure 9b which shows that the two contact zones are at ambient temperature possibly due to conduction heat transfer.

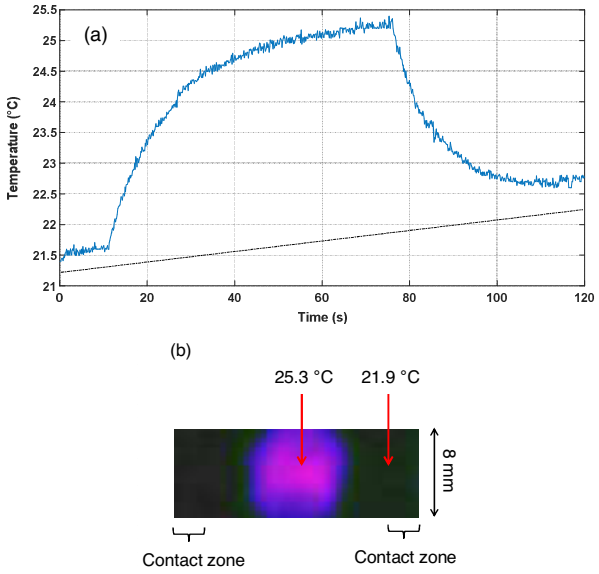

Fig. 9. a) Temperature change of the PyC surface when it is illuminated by a laser beam of wavelength 1064 nm and optical power P_{irr} of 0.9 W for 60 s. Dotted line is the air temperature mean value near the PyC sheet.
b) False color image of the PyC surface after 60 s irradiation.

Figure 10 shows the simultaneous measurements without laser irradiation of mass change 10(a) and air temperature close to the pan 10(b) over 250 min. In order to reduce the influence of air-conditioning system, an enclosure made of transparent plastic has been installed to protect the entire set-up (except the laser) against air movement. The two blue curves 10(a) and 10(b) recorded before the enclosure was installed are clearly correlated. There are large oscillations with a period of about 60 min due to air-conditioning control. The two signals are in opposition of phase. The peak-to-peak amplitudes are about 0.5 °C and 1.8 mg for air temperature and mass changes respectively equivalent to a temperature sensitivity coefficient of -3.6 mg·°C^{-1}. The oscillations are not symmetrical. The maximum positive mean slope (considering the large oscillations) is about +0.12 mg/min and the minimum negative mean slope is about -0.05 mg/min for the mass change.

 DOI: 10.1051/metrologie/201717001

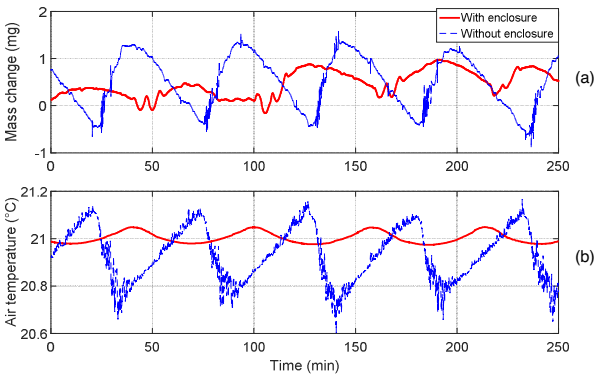

Fig. 10. Measurements without the transparent plastic enclosure (blue curves) and with the enclosure (red curves) over 250 min of: (a) Mass change (without laser irradiation); (b) Ambient air temperature close to the pan.

The amplitude of 1.8 mg observed without the plastic enclosure cannot be explained by the buoyancy change using expressions (4) and (5) giving a temperature sensitivity coefficient of +0.24 mg·°C^{-1}. This effect is of opposite sign and too small compared with the measured temperature sensitivity coefficient.

Another origin might be the magnetic induction variation with temperature. Considering that the manufacturer of NdFeB magnets gives a typical remanent induction B_r of 1.2 T (independent of the magnet's geometry) and that the temperature coefficient of remanence ζ is -0.1 % °C^{-1} for NdFeB magnets, an approximate calculation has been carried out to verify this assumption.

In our experiment as shown in the previous paper [1], the magnetic flux density in an x-y plane at the height z above the magnet array exhibits a 2D periodicity due to the magnet array composed of a juxtaposition of small identical permanent magnets in a horizontal plane x-y. In this case, the vertical induction component B_z has a horizontal periodic and homogeneous distribution. Its mean value in the horizontal plane is constant. In these conditions, a variation of temperature ∂T involves a variation of magnetic induction $\partial B_r = B_r\, \zeta \partial T$. This leads to an approximate derivative of magnetic induction related to temperature $\partial B_r/\partial T$ of about -10^{-3} T·°C^{-1}.
We can use the following approximate expression for the magnetic force acting on the PyC sheet:

$$F_z \approx -\chi . \frac{S}{\mu_o} . \int_z B \frac{\partial B}{\partial z} . dz \qquad (7)$$

where μ_0 is the vacuum permeability ($4\pi\times10^{-7}$ H·m^{-1}), χ the volume magnetic susceptibility of pyrolytic carbon (-4×10^{-4}) and S the base area of the PyC sheet (192 mm^2).

The expression to calculate the magnetic flux density B_z of a cylinder magnet of diameter and height $2R$ at the distance z from a pole face on the symmetrical axis is as follows:

$$B_z \approx \frac{B_r}{2}\left[\frac{2R+z}{\sqrt{R^2+(2R+z)^2}} - \frac{z}{\sqrt{R^2+z^2}}\right] \qquad (8)$$

Considering that the levitation force F_z acting on the PyC sheet at z = d_0 ≈ 0.4 mm for m_0 = 0.41 g is about 4 mN and that expressions (7) and (8) lead to the following expression:

$$\frac{\partial F_z}{\partial T} \approx 2\frac{F_z}{B_r}\frac{\partial B_r}{\partial T} \qquad (9)$$

we obtain from expression (9): $\partial F_z/\partial T$ = -73×10^{-6} N·°C^{-1}. We deduce an approximate mass variation ∂m=-3.7 mg for ∂T=+0.5 °C. Although this result is somewhat twice as large as the measured mass change of -1.8 mg, it corresponds to a temperature sensitivity coefficient $\partial m/\partial T$= -7.5 mg·°C^{-1} of the same sign as -3.6 mg·°C^{-1}.

Figure 10 (red curves) shows the efficiency of the plastic protection. The peak-to-peak amplitude of air temperature close to the balance pan is about 0.08 °C compared with 0.5 °C without enclosure. One can observe a temperature change period of about 60 min, but the correlation between variations of temperature and mass is much less clear because of other small disturbances of almost the same amplitude (gentle movement of air, vibrations, instability of servo-control…). Note that the maximum mass oscillation amplitude is about 0.5 mg and that the oscillations between temperature and mass measurements are of opposite phase. In addition, we observe also a double oscillation (period of about 6.5 min and amplitude of about 0.3 mg) on the mass change curve after each maximum temperature corresponding to a maximum of the second time derivative of temperature d^2T/dt^2 possibly coming from the servo-control system of the mass comparator.
A correction of air temperature based on the linearization of temperature change over t_{max} has been applied on mass change measurements using a Matlab® program.

3.4 Results and discussion

In this configuration, we observe a delay time of several seconds. In order to reduce the measurement time and to take into account the delay time, we choose to determine a response time τ as the time to reach 1/e of the mass change value at t_{exp} when t_{exp} corresponds to the time to reach a quasi-extremum level (quasi plateau).

 DOI: 10.1051/metrologie/201717001

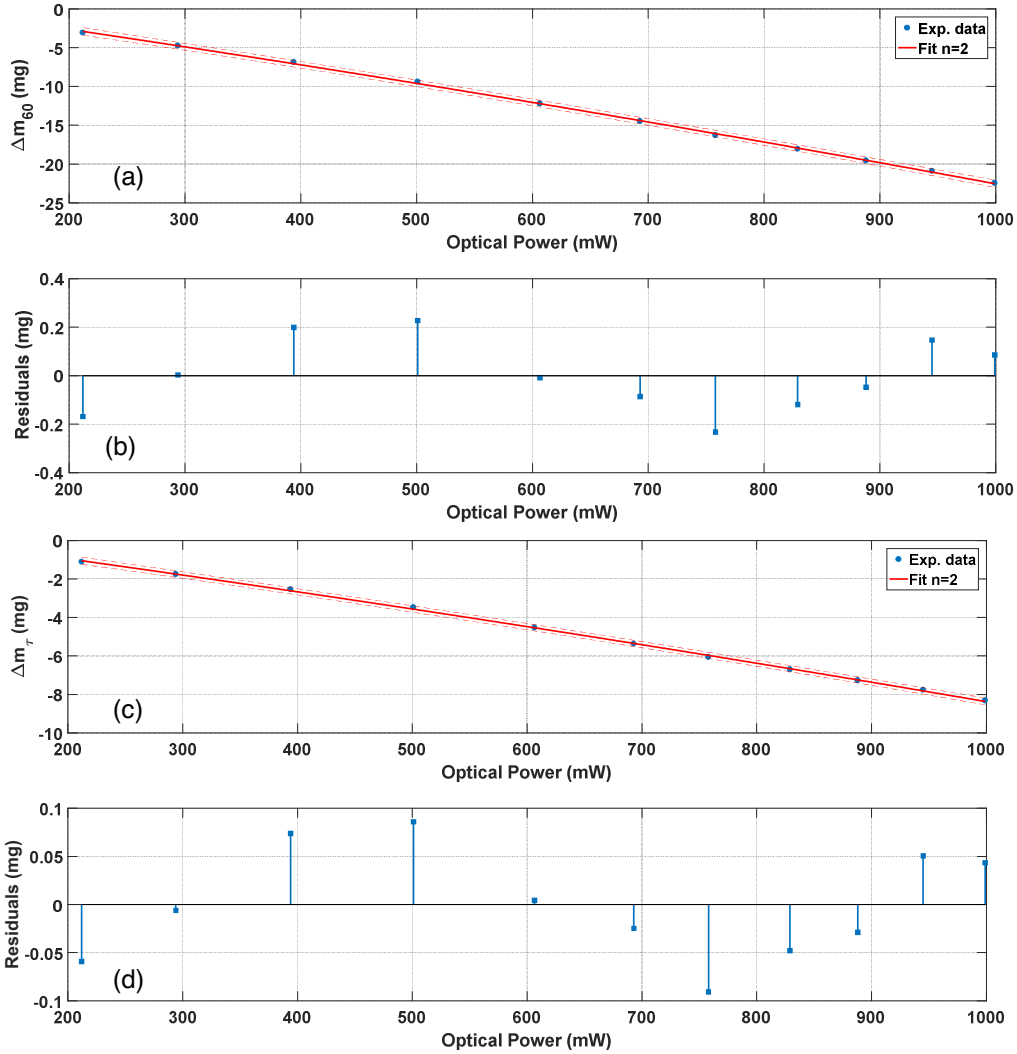

Fig. 11. Mass measurements for four increasing and decreasing (ID) optical power values P_{irr} between 200 and 1000 mW generated by the laser of wavelength 1064 nm: (a) maximum mass changes Δm_{60} after a 60 s exposure time (t_{exp}); (b) residuals of Δm_{60} for a second-order polynomial fit; (c) mass change Δm_{τ} at τ; (d) residuals of Δm_{τ} for a second-order polynomial fit.

Figure 11a shows an example obtained from experimental mass changes for four increasing and decreasing optical power values P_{irr} between 200 and 1000 mW generated by the laser of wavelength 1064 nm with an exposure time of 60 s. This example is not one of the best in terms of linearity. Even a second-order polynomial fit gives residuals (Fig 11b) which are not negligible, *i.e.* about 2%. Figure 11c shows the mass changes at τ determined from the measurements in Figure 11a. The response time is about 7.5 s while the delay time is about 2.5 s. In this case, residuals of the second-order polynomial fit reach about 3%. In better adjustment conditions of the experimental device, we obtained a linearity error less than ±1% over a sub-range 400 mW – 1000 mW.

These results show that there is no significant hysteresis phenomenon and that the relative measurement reproducibility is less than 0.4%.

A correction of the temperature drift is applied on experimental mass changes. However, the effect of this correction is weak enough.

We have demonstrated [2] that the relative uncertainty of optical power measurement with this set-up in the range 400 mW-1000 mW at 1064 nm spreads from 1.6% to 0.8% and that the irradiating beam wavelength (532 nm and 1064 nm) affects the photo-response of pyrolytic carbon.

In addition, Table 1 shows the device is able to measure low optical powers around 20 mW at 532 nm for an exposure time of 120 s. The delay time is about 20 s and the discrimination threshold smaller than 1 mW.

Table 1. Statistical parameters (mean associated with standard deviation) for three measurement parameters determined from a series of five records for three optical powers P_{irr} at 532 nm. The differences of the mean values between 15.3 mW and 17.5 mW and between17.5 mW and 19.5 mW are determined.

Optical power (mW)	Statistical parameters	τ (s)	Δm_τ (mg)	Δm_{120} (mg)
15.3 (a)	mean	35.86	-0.2412	-0.652
	standard deviation of mean	0.39	0.0061	0.016
	relative standard deviation (%)	1.1	2.6	2.5
17.5 (b)	mean	36.12	-0.2829	-0.766
	standard deviation of mean	0.25	0.0061	0.016
	relative standard deviation (%)	0.7	2.2	2.1
19.5 (c)	mean	36.56	-0.3261	-0.8674
	standard deviation of mean	0.13	0.0024	0.00059
	relative standard deviation (%)	0.4	0.7	0.7
(a-b)	mean difference	-0.26	0.0417	0.114
	standard deviation	0.46	0.0086	0.023
	relative standard deviation (%)	177	21	20
(b-c)	mean difference	-0.44	0.0432	0.101
	standard deviation	0.28	0.0066	0.016
	relative standard deviation (%)	64	15	16

4 Conclusion

We have demonstrated that an elementary device consisting of a small plate of pyrolytic graphite levitated above a magnet array is sensitive to a laser power. This leads to an interesting alternative to power meters based either on thermal measurement techniques via the Stefan-Boltzmann law (absorbed energy related to a temperature increase) or on the photon-electron interaction (photodiode effect).

Two different experimental configurations were studied.

The levitation configuration is quite compact but very sensitive to ground vibrations, draughts and ambient temperature changes. The photo-response sensitivity of the experimental set-up is at least 100 $mW \cdot \mu m^{-1}$ for most positions of the PyC sheet, but it is not linear over the whole range 100-1000 mW. Its discrimination threshold is about 3 mW and the relative measurement uncertainty of optical power in the range 100-1000 mW at a wavelength of about 1 µm is less than 10%.

The weighing configuration is also sensitive to ambient temperature changes. A temperature correction can be applied. In this configuration, there is a delay time of several seconds which is not negligible. The discrimination threshold is smaller than 1 mW. As with the levitation configuration the photo-response is also not linear over the whole range 100-1000 mW. The relative measurement uncertainty of optical power in the range 400-1000 mW at a wavelength of about 1 µm is less than 2%.

First results are very encouraging. This confirms the feasibility of new laser power sensors using diamagnetic repulsion which look promising for applications in metrology, in industry or in technology development.

Many features of these PyC-based devices could be improved. For instance, we are currently studying a new design of PyC-based sensors for industrial lasers of about 1 kW. Its principle consists in splitting off only a few percent of the laser power and using a chopper alternating short irradiation and long darkness periods. Such a device could measure a laser power with a relative uncertainty better than 10 %. Although the response time is several seconds, it could be integrated into a real-time system to monitor and control laser powers used in industry. Moreover, in the levitation configuration, a damping system against ground vibrations and a servo-control system of the magnet array temperature using a Peltier module are currently being tested. Ultimately, the best possible improvement would consist in linking the photoresponse to irradiating optical power by a physical law deduced from the optical and electronic properties of PyC. In this case, PyC-based devices could be used as absolute measurement standards.

The authors thank Dr Mark Plimmer for helpful discussions.

References

1. P. Pinot and Z. Silvestri, New laser power sensor using diamagnetic levitation (submitted in *Review of Scientific Instruments*)
2. P. Pinot and Z. Silvestri, New laser power sensor using weighing method (submitted in *Measurement Science and Technology*)
3. P. Williams, B. Simonds, J. Sowards and J. Hadler, Proc. SPIE 9741, *High-Power Laser Materials Processing: Lasers, Beam Delivery, Diagnostics, and Applications V*, 97410L (2016)
4. M. Kobayashi and J. Abe, J. Am. Chem. Soc, **134**, 20593-20596, (2012)
5. JCGM 100:2008, First edition 2008, Corrected version 2010, BIPM.
6. *Organisation internationale de métrologie légale* (OIML): *Weights of classes E1, E2, F1, F2, M1, M1−2, M2, M2−3 and M3: part I. Metrological and technical requirements*, International Recommendation OIML R 111, 2004 (Paris).